World Applied Sciences Journal 6 (9): 1287-1297, 2009
ISSN 1818-4952

Transient Performance Prediction of Transformers by a Nonlinear Multi-values Hysteresis Model of Priesach

Ahmad Darabi, Mohsen Khosravi

Faculty of Electrical and Robotic Engineering Shahrood University of Technology, Shahrood, Iran

Abstract: Magnetic characteristics of the iron cores affect significantly the steady and transient performances of the transformers. Due to nonlinear and multi-values characteristics, modeling of the hysteresis behavior of a magnetic material is principally complicated. In general the conventional methods yield to inaccurate results, particularly when are employed to model a transient phenomena. Scalar model of Priesach is a powerful numerical method and might be applied for modeling of a transformer core with some confidences. However, programming the Priesach model coupled with external circuits of a transformer is somewhat complicated and needs a further considerations and proper less time-consuming computational algorithm. In this paper, a comprehensive computerized model of a transformer core combined with winding details and electric equations of the terminals is presented. The numerical problems associated with implementation of the transformer model using Priesach model are reduced greatly by the suggested algorithm. That provides completed information regarding all electric and magnetic quantities of the transformer including the instantaneous voltages and currents, flux density and field intensity. Therefore by use of the proposed model, one can evaluate the steady state and transient performance of a transformer and specify for example the terminal parameters and degree of core saturation.

Key word: Hysteresis . nonlinear model . priesach model . transformer . transient

INTRODUCTION

Along with progress in power system studying, accurate modeling and performance analysis of transformer as an important component of the power system have taken extensive attentions. Furthermore small transformers are in used in the power sections of many devices. Therefore from different points of view an accurate model of transformers is essential. Some transient performances of a transformer e.g. inrush currents may damage the power system components or cause miss-function of relays and protection equipments. Transformers employed in the power sections of commonly electronic devices affect the harmonic content and other power quality characteristics of the voltages and currents. These type studies cannot be lead to an accurate result without taking hysteresis phenomena of the iron cores into account.

Various models have been suggested for simulating and then analyzing of a transformer behavior. These modeling approaches were classified into three categories [1]:

- Matrix representation is just developed for a linear model and the excitation effect is appeared in the output terminal of a non-linear element (Fig. 1). This model may give an acceptable result for an event with the harmonic content frequencies lower than 1 kHz [2].
- A transformer with less than three windings can be represented by a saturable transformer component with a star-circuit [1, 3, 4]. In this model a non-linear inductance might be located in the beginning of the model as shown in Fig. 2.
- The third group is topology based models that are divided into two subgroups. a) The models which are based on duality. In this method, the transformer model is gained by the circuit approach without any mathematical description and b) Geometric models in which the mathematical descriptions are obtained by coupling the magnetic equations of the core topology to the electrical equations of the machine [5, 6]

Among these categories the topology based modeling approaches are regarded as the most informative. In 1981, Deak and Watson presented a three-legged stocked core model of transformer [7]. They suggested a new valuable experimental model for the hysteresis and a method to determine the transformer parameters by use of measurement results.

Corresponding Author: Dr. Ahmad Darabi, Shahrood University of Technology, Faculty of Electrical and Robotic Engineering, 7Th Teer Square, P.O. Box 36155-316, Shahrood, Iran

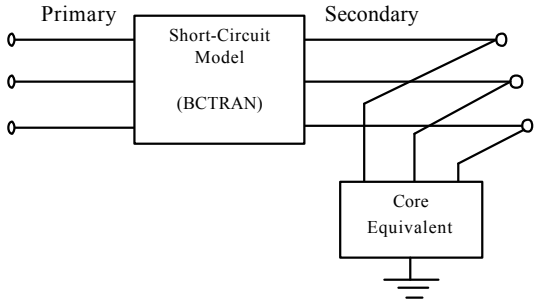

Fig. 1: BCTRAN-based model [1]

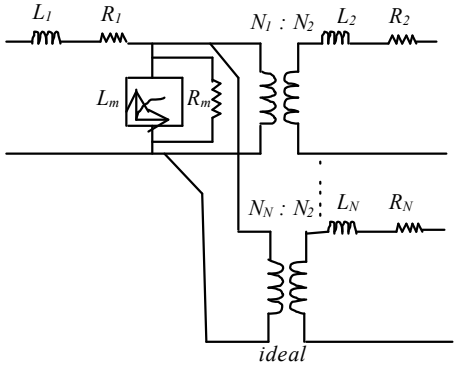

Fig. 2: STC Model of single-phase [1]

In 1991, this technique was applied for five-legged step-up transformer working in highly saturated condition by Arturi *et al*. [8]. In 1994, De León and Semlyen proposed a rather completed model for the transformers. This modeling approach employs a hybrid method for gaining the iron-core model and calculating the leakage inductance [9]. Narang and Brierley in 1994 applied the duality principle and got an equivalent circuit for the transformers. In their model the equivalent magnetic circuit model is connected to the admittance matrix through three-phase artificial windings [10]. In 1999 Mark and *et.al* presented a five-legged wound transformer core model that was used to analyze the ferroresonant phenomena [11]. All the models mentioned above can be accounted as topology-based models and belong to the first subgroup. Some other models related to the topology-based models, have been proposed. For example, Yacamini and Bronzeado developed a magnetic coupling model which is used to simulate the transient state specially the inrush current. In this model the connection between the magnetic and electrical equations is made by Ampere's law [12]. In addition, a magnetic equivalent circuit model has been proposed by Arrillaga in which the leakage parameters are obtained through open circuit and short circuit experiments [13]. Another model named GMTRAN has been developed by Hatziargyriou *et al*., in which the equations are defined as $[\lambda] = [L][I]$. Finding the matrix [L] is the main point in the model [14]. In the SEATTLE XFORMER_ model developed by Chen, flux linkage is considered as a state variable [15].

However, the conducted researches applying the hysteresis behavior of iron core in the magnetic and electrical equations of transformers are not too many. In reference [16], an equivalent circuit consists of a resistance and a constant inductance in series is used. In which, the resistance value is obtained by equating power loss with real iron loss. In this model, the circuit equations are combined with the modified model of Langevin given for the magnetization as

$$M = M_S(\coth\frac{H_L + \alpha_m}{A} - \frac{A}{H_L + \alpha_m})$$

This model is just limited to the low frequencies and accuracy of the model decreases when the core becomes close to the saturation condition where the approximation used in the model as

$$\frac{dM}{dH_L} + 1 \cong \frac{dM}{dH_L}$$

is not further valid. Moreover, Langevin model defined by *tanh* or *Arctan* functions in cases in which the core magnetization curve, wherein gently drawing on the saturation, is much wider than the area drawing on the saturation abruptly, have some problems.

Perhaps, we can claim that one of the best techniques for modeling the magnetic cores and residual behavior has been proposed by Preisach [17]. Classical Preisach Model (CPM) of the ferromagnetic materials was first introduced by Ferenc Preisach and afterward it became a basic for all Preisach models. Filip *et al*. in 1994 described the Preisach model under classical conditions that there was a logical adaptation between the classical model of Preisach and the experiments conducted on the silicon laminations. Recently, many efforts have ever made by Mayergoyz for developing the Preisach model in both scalar and vector modes [17]. This model has been used for various calculations of electrical and mechanical systems. For instance, article [18] indirectly used this model to calculate the local iron loss of a synchronous machine. But, not many experiments for applying the Preisach model directly to the real systems like transformers have been conducted. Therefore the problems occurred in applying the Preisach model to a transformer coupled to the external circuits have been remained unsolved. These problems are due to the difficulties such as being multi-inputs, too many

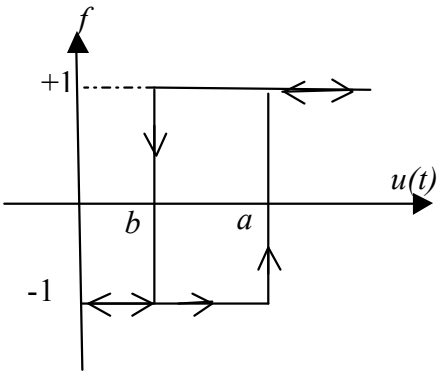

Fig. 3: Delay component

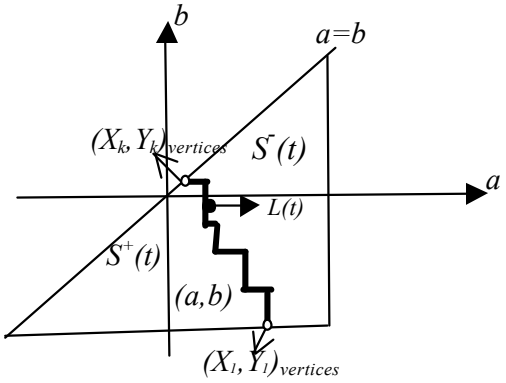

Fig. 4: Preisach triangle

constraints, non-linearity, multi-value nature and time-consuming computation process.

In this paper using the Preisach model, we proceed to take the hysteresis behavior of the core into account while formulating the magnetic and electrical equation of a transformer. The problems associated with applying the Preisach model to a transformer are investigated and a comprehensive algorithm for calculating the transformer performances in both steady and transient state is given. Using this computerized model, almost all of the transformer phenomena such as inrush currents and ferroresonance phenomenon can be studied with some accuracy.

Preisach model: In the recent years, Preisach model has been developed in both scalar and vector modes for describing the hysteresis phenomenon. In the steady state, the magnetization of a ferromagnetic material in a periodic sinusoidal or non-sinusoidal magnetic field can be easily calculated by a delay component. This delay component is simply shown in Fig. 3 in which the relation between an input variable u(t) and an output variable f(t) is as:

$$\begin{aligned} &f(t)=1 \quad \text{if} \quad u(t)\geq a \\ &f(t)=-1 \quad \text{if} \quad u(t)\leq b \\ &f(t)=\text{unchanged} \quad \text{if} \quad b<u(t)<a \end{aligned} \tag{1}$$

Let us introduce the operator $\hat{\gamma}_{ab}$ as it operates on input H(t) and gives f(t). If we suppose that there is infinite number of these delay functions with the same operators for a random point of the magnetic material, so the output of this set will be as:

$$M(t)=\iint_{a\geq b} p(a,b).\hat{\gamma}_{ab}.H(t)\quad dadb \tag{2}$$

Where p(a,b) is named the density function. Preisach operator has a local memory with specific values of maximum and minimum. For a homogeneous magnetic material, the field intensity in which saturation occurs is denoted by H_s. Therefore if $a>H_s$ or $b<-H_s$ then $p(a,b) = 0$ and the Preisach triangle shown in Fig. 4 is defined as:

$$S^{\Delta}(t)=\{(a,b)|a\geq b, b\geq -H_s, a\leq H_s\} \tag{3}$$

For each point $(a,b)\in S$, there is an operator similar to $\hat{\gamma}_{ab}$ and for a given time t, the S plot is divided into 2 parts:

$$\begin{aligned} S^{+}(t)&=\{(a,b)\in S|\text{output of } \hat{\gamma}_{ab} \text{ at t is } +1\} \\ S^{-}(t)&=\{(a,b)\in S|\text{output of } \hat{\gamma}_{ab} \text{ at t is } -1\} \end{aligned} \tag{4}$$

At any time t, $S(t)=S^{+}(t)\cup S^{-}(t)$ and the equation (2) can be rewritten as:

$$M(t)=\iint_{S^{+}(t)} p(a,b)dadb-\iint_{S^{-}(t)} p(a,b)dadb \tag{5}$$

At a time t, the Preisach plane is divided into the high switching field S^{+} and low switching field S^{-}. While the input H increases, a vertical line sweeps the Preisach plane from left to right and when H decreases, a horizontal line sweeps the plane up to down. If H with a limited number of local extremum varies between-H_s and H_s, obviously M would change between M_s and-M_s. Therefore, we can easily prove that the density function should satisfy the equation given as:

$$\iint_{S(t)} p(a,b)dadb=2M_s \tag{6}$$

So the equation 5 can be rewritten as:

$$M(t)=-M_s+2\iint_{S^{\wedge}(t)} p(a,b)dadb \tag{7}$$

Table 1: optimum parameters of density function for LOSIL_630

Section	a and b values	$10^{-4}m_{ss}$	s_1	s_2	u_c
1	-100 < b,-100 < a <100	74.49167	70.23533	67.95768	80.960259
2	except section no. 1-112 < b,-112 < a <112	73.50453	43.63087	60.24348	83.67477
3	except sections with no. less than 3-122 < b,-122< a <122	88.91253	69.66376	46.45285	80.73351
4	except sections with no. less than 4-132 < b,-132 < a <132	91.89059	64.69753	42.70985	89.04827
5	except sections with no. less than 5-142< b,-142 < a <142	80.90639	35.17563	52.05150	105.68034
6	except sections with no. less than 6-154< b,-154 < a<154	78.92915	6.87975	66.51201	108.94130
7	except sections with no. less than7-168< b,-168< a<168	86.45607	53.81372	61.29249	118.11890
8	except sections with no. less than 8-188< b,-188 < a <188	79.55638	57.66232	32.03302	109.73872
9	except sections with no. less than 9-216<b,-216 < a < 216	68.13034	32.47861	63.97896	117.00194
10	except sections with no. less than 10-266<b,-266< a<266	75.53657	43.29980	82.04428	132.48656
11	except sections with no. less than 11-346<b,-346 < a < 346	117.96480	105.06150	64.73821	111.74766
12	except sections with no. less than 12-500<b,-500 < a<500	115.02650	98.38718	119.95690	143.26790
13	except sections with no. less than 13-880<b,-880<a< 880	165.39780	251.85880	78.83422	131.25544
14	except sections with no. 1 to 13	259.73530	421.63570	129.47513	215.13744

By calculating M using equation 7, we can compute the flux density B of a given point by [17]:

$$B(t) = \mu_0\{H(t) + M(t)\} \quad (8)$$

Where $\mu_0 = 4\pi\times 10^{-7}$.

SIMULATION OF THE PREISACH MODEL

While ferromagnetic material is exposed to a periodic symmetric field with a specified peak value, the magnetization and the steady-state flux density of each point of the material can be calculated by one-dimensional Preisach model. In fact, the number of broken lines shown in Fig. 4 at the boundary of S^+ and S^-, illustrates the number of local extremum of magnetic field, since last absolute extremum until present time. Knowing the vertices of the broken lines up to the time t, the value of M and then B can be determined for the time $t+\Delta t$ by a computer simulation. The program examines whether the value of $H(t+\Delta t)$ is more or less than H(t) and then calculates the values of M and B using equations 7 and 8. After these calculations, new vertices of cursives in the border of S^+ and S^- for the time $t+\Delta t$ can be determined.

Density function: The steel lamination employed as a core for the transformer of the present paper is LOSIL-630. Four descriptive parameters of two-variable density function of the material have been already determined precisely using the experimental results by reference [18].

Parameters of the multi-equation function are given in the Table 1.

General form of the density function is:

$$2p(a,b) = \frac{m_{ss}}{\pi\sigma_1\sigma_2}\exp\left(-\frac{(a+b)^2}{4\sigma_1^2} - \frac{(a-b-2u_c)^2}{4\sigma_2^2}\right)$$

Where four parameters

σ_1, σ_2, σ_c, u_c and m_{ss} are different for various materials and areas of the Preisach triangle. As mentioned earlier, these variables are determined using the experimental B–H and iron loss per kilogram characteristics of the material given by manufacturers and the best curve fitting approach. For more details see reference [18].

Initial conditions: Firstly specifying the initial values of H and B is necessary. In fact absolute minimum and the broken lines of the Preisach triangle or the vertices are needed for simulating a transformer. If the initial values of H and B are zero, to determine properly the vertices of the Preisach triangle, the symmetric characteristic of the density function with respect to the line a =-b line is used to determine the vertices. It is essential to choose too many vertices of Preisach triangle as far as possible near to the line a =-b to achieve zero conditions for magnetic core. In a real experiment to achieve the zero condition for a magnetic core ($H\cong 0$, $B\cong 0$), i.e. omitting the residual flux density of the core, we should apply a slowly vanishing sinusoidal voltage to eliminate the magnetic field of the core. Figure 5 and 6 will completely show the movement on the loops and reaching to the zero point. To reach the zero residual condition it is essential to apply sinusoidal voltage with low frequency vanishing amplitude (e.g. *5 Hz*). In fact, each extremum of H plot produces a breakage at the boundary of S^+ and S^- in the

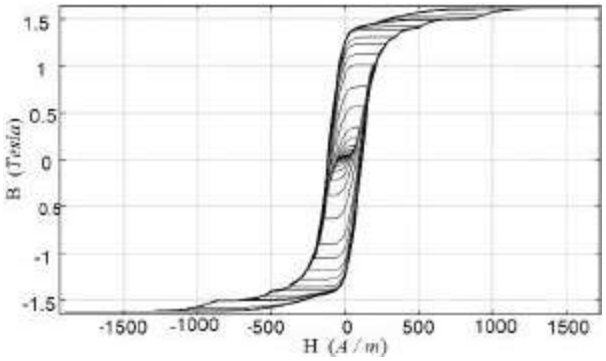

Fig. 5: B-H curve while core is becoming close to point of H=0 & B=0, by applying vanishing magnetic field

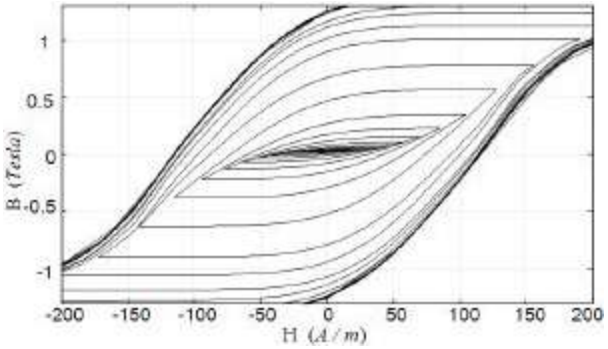

Fig. 6: Enlargement of Fig. 5

Preisach plane. Therefore all vertices of Preisach plane (Fig. 7) are related to the returning points of the hysteresis loops in the second and fourth quadrant (Fig. 5 and 6).

DISCRETE MODEL OF TRANSFORMER AND LOAD

Simulated system in this paper consists of a small experimental transformer that primary and secondary are connected via transmission lines to a power supply and load as shown in Fig. 8. Design details of the transformer are given in Table 2. Resistances and inductances of the transmission lines are:

$$R_{Line1} = 8.3e-03, L_{Line1} = 8.3e-06, R_{Line2} = 0.05$$

and $L_{Line2} \cong 0$ per unit.

The system equations in a discrete form can be written as:

$$V_1(t) = (R_{T1} + R_{Line1}) I_1(t) + (L_{T1} + L_{Line1}) \frac{dI_1(t)}{dt} + N_1 A_c \frac{dB(t)}{dt} \quad (9)$$

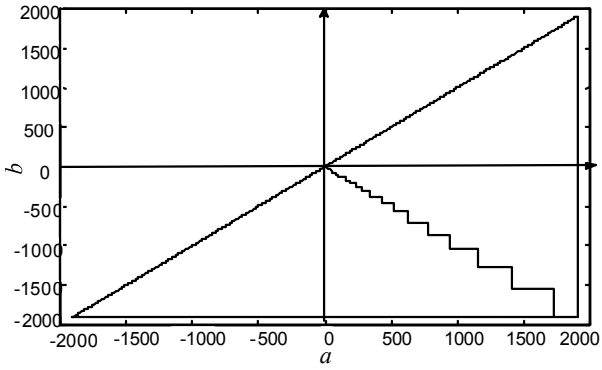

Fig. 7: Triangle Preisach after applying a vanishing magnetic field (Each breakage is associated with an extermum)

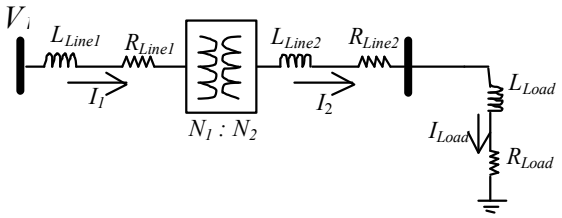

Fig. 8: Simulated system

$$N_2 A_c \frac{dB(t)}{dt} = (R_{T2} + R_{Load}) I_2(t) + (L_{T2} + L_{Load}) \frac{dI_2(t)}{dt} \quad (10)$$

$$H(t) = \frac{N_1}{l_c} I_1(t) - \frac{N_2}{l_c} I_2(t) \quad (11)$$

$$B(t) = \text{Preisach}(H(t), H(t - \Delta t)) \quad (12)$$

where A_c and l_c are the cross-section and average length of the core, N_1 and N_2 are the numbers of turns of primary and secondary windings, R_{T1} and L_{T1} are the resistance and the leakage inductance of the primary side while R_{T2} and L_{T2} are the resistance and the leakage inductance of the secondary respectively.

Equations 9 to 12 can be illustrated by block diagrams of Fig. 9 in which,

$$R_1 = R_{T1} + R_{Line1}$$

$$L_1 = L_{T1} + L_{Line1}$$

$$R_2 = R_{T2} + R_{Line2}$$

and

$$L_2 = L_{T2} + L_{Line2}$$

However for solving the equations, we use the Rang-Koutah method so the discrete equations are rewritten as follows:

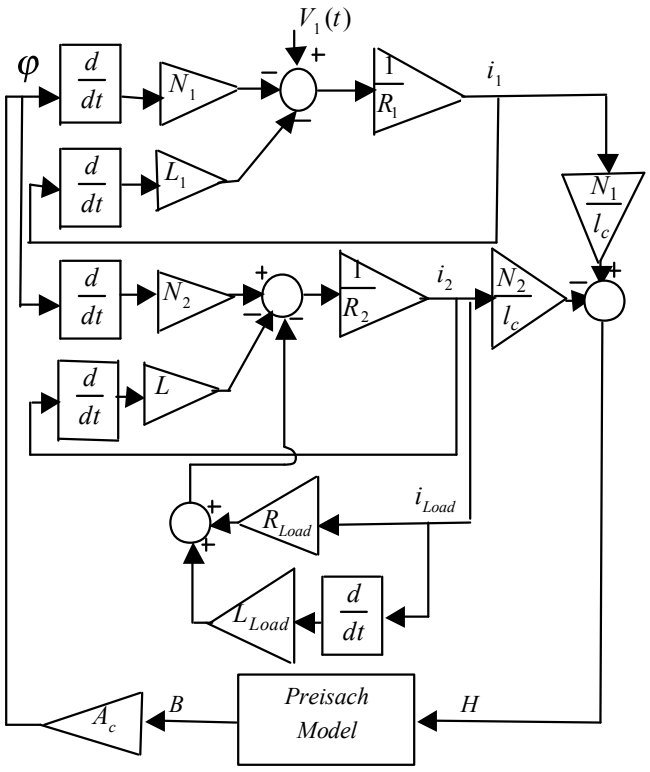

Fig. 9: Simulation block diagram of the system shown in Fig. 8

$$\left(\frac{V_1(t+\Delta t)+V_1(t)}{2}\right)\Delta t-(R_{T1}+R_{Line1})\left(\frac{I_1(t+\Delta t)+I_1(t)}{2}\right)\Delta t \\ -(L_{T1}+L_{Line1})(I_1(t+\Delta t)-I_1(t))-N_1A_c(B(t+\Delta t)-B(t))=0 \quad (13)$$

$$N_2A_c(B(t+\Delta t)-B(t))-(R_{Load}+R_{T2})\left(\frac{I_2(t+\Delta t)+I_2(t)}{2}\right)\Delta t \\ -(L_{T2}+L_{Load})(I_2(t+\Delta t)-I_2(t))=0 \quad (14)$$

$$l_cH(t+\Delta t)-N_1I_1(t+\Delta t)+N_2I_2(t+\Delta t)=0 \quad (15)$$

$$B(t+\Delta t)=\text{Preisach}(H(t+\Delta t),H(t)) \quad (16)$$

Having the system parameters and the input voltage of the power supply, the final goal of solving the equations set (13 to 16) can be the instantaneous values of the currents. However for this purpose the instantaneous values of the magnetic field intensity and flux density must be computed. The main problem is commonly time-consuming numerical method hired to gain the system response. The Preisach model is the most time consuming blocks of the whole simulations. Therefore, to reduce the computation times and to avoid divergence problem of the iterative methods, instead of moving on 't' axis with specified time step Δt, we can move on the H axis with intelligent step size of ΔH and solve the equations by assuming a known value for $H(t+\Delta t)$. At any time 't', the values of $I_1(t)$, $I_2(t)$, H (t) and B (t), are assumed known. Applying an initial guess for the value of $H(t+\Delta t)$ (a value closed to the value of H(t)) the value of $B(t+\Delta t)$ is evaluated by the Preisach model. After that, the unknown variables, comprising Δt, $I_1(t+\Delta t)$ and $I_2H(t+\Delta t)$ are computed using equations 13 to 15. The calculated value for Δt has to be positive, real and small, otherwise, the value of $H(t+\Delta t)$ should be revised properly. The way of revising the value of $H(t+\Delta t)$ is a key point. The flowchart of the proposed algorithm is illustrated in Fig. 7. At the beginning of the simulation, the initial values of currents, H and B are assumed known. The value of H and B are related to the vertices of Preisach triangle (defined as $(X, Y)_{vertices}$) in the boundary of the areas S^+ and S^-.

In the algorithm, to determine the ascending or descending trend of H, a variable named *check* is

Table 2: Transformer details

Primary winding resistance (R_{T1})		0.07 p.u
Primary leakage inductance (L_{T1})		8.5e-05 p.u.
Number of the primary winding turns		433 turns
Secondary winding resistance (R_{T2})		0.25 p.u.
Secondary leakage inductance (L_{T2})		2.3e-3 p.u.
Number of the secondary winding turns		77 turns
Core dimensions	Design type	EI 150N
	A_c	24 cm^2
	L_c	35 cm

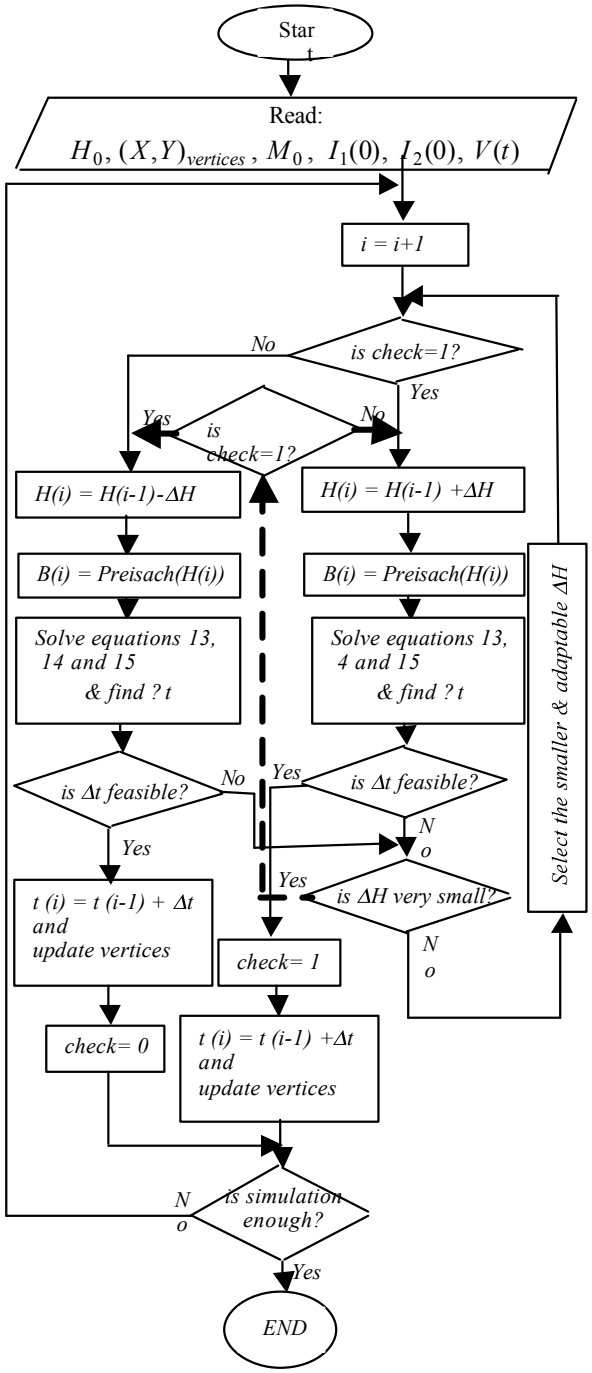

Fig. 10: Simulation Algorithm

defined. If the value of *check* is 1 then H is increasing and commonly except in the returning point we should add a positive value such as ΔH to H in order to get a proper value for H(t+Δt) otherwise, if the value of *check* is zero we must subtract ΔH from H and get a value for H(t+Δt). As it can be been seen from the flowchart, for adapting the flowchart with the programming languages, arrays are used. For example, H(i-1) and H(i) are employed instead of H(t) and H(t+Δt) respectively. In each time, we suppose that H has its own previous increasing or decreasing mode, so, the value of H(t+Δt) is chosen as H(t)+ΔH or H(t)-ΔH depending on the value of the variable *check*. By determining the values of H(t+Δt), H(t), B(t) and knowing the vertices of Priesach triangle until present time, it can be possible to calculate B(t+Δt) using Preisach model. Knowing the values of H(t), H(t+Δt), B(t), B(t+Δt), $I_1(t)$ and $I_2(t)$, equations 13 to 15 will be three equations with three unknown variables Δt, $I_1(t+\Delta t)$ and $I_2(t+\Delta t)$.

For solving the three non-linear equations, the Matlab command named *'fsolve'* is used. As mentioned early, when the calculated value for Δt is positive, real and small, it would be acceptable, otherwise, the value of H(t+Δt) has to be modified. Getting an unacceptable value for Δt can be due to either a great value of ΔH or presumed value of the variable *check* (returning point). In this case firstly, we suppose that ΔH is too big so, some lower values for ΔH are applied and the calculations are repeated until the given criterion is satisfied. If these calculations do not converge to an acceptable response until a pre-determined small value of ΔH, undoubtedly, the problem is due to the presumed increasing or decreasing mode of H. This situation is happened just in the returning points. However in this case, by altering the value assigned to the variable *check*, the calculations are repeated until an acceptable value for Δt is achieved. When this condition is satisfied the calculations for this time are finished so the coordinates of vertices ($(X, Y)_{vertices}$) are updated and calculations for a newer time are begun.

Using the proposed algorithm, divergence and the problems associated with long computation time of routine way of solving equations 13 to 16 are significantly reduced. As mentioned previously calculation of variable B(t+Δt) using the Preisach model are complicated and time consuming. Therefore the advantage of the suggested method is obviously referring to the Preisach model once or rarely twice for each time step calculations to get the value of unknown variables. On the contrary, if the classic method is used referring to the Preisach model would be repeatedly necessary for each time step calculations and this required a huge computer time for a few cycle calculations.

SIMULATION RESULTS

The system introduced previously is simulated under various loads. As an example, the simulation results for an inductive load with $R_{Load} = 0.5$ p.u. and

L_{Load} = 1.25e – 04 p.u. are presented. A voltage source as $V_1(t) = 220\sqrt{2}\sin(100\pi t+\varphi)$ is applied to the beginning terminals of the transmission line.

This system is chosen just as an example to illustrate the capability of the proposed modeling approach. The initial value of the voltage source at the time of switching is a most effective parameter on the transient performance of the transformer investigated in this paper. Various initial values of the voltage at the time of switching can be produced by choosing different values for the phase angle φ of the voltage source. For briefness only the simulation results for two extreme conditions i.e. for zero ($\varphi = 0$) and maximum ($\varphi = \pi/2$) initial voltage are illustrated and analyzed. The simulations are carried out when the transformer has been already connected to the load and switching to the voltage source is done in the primary side of the transformer.

Different simulation results of the transient performance for $\varphi = 0$ are illustrated in Fig. 11-19. Transient and steady state B-H curves are shown in Fig. 11-13 whereas Fig. 11 shows the whole transient B-H curve, Fig. 12 is an enlargement of Fig. 11 partially and Fig. 13 is the last loop of Fig. 11 and 12 illustrating the steady state B-H loop. As seen from these figures, for some durations of time at the beginning of transient, the hysteresis loops are asymmetric around the origin, but, slowly become symmetric until the steady state that a full symmetric loop is achieved. Also, transient response of the field intensity given in Fig. 14 show that at the first two half period of the beginning of the transient, the magnitude of H is increased significantly and then is decreased rapidly until the following steady state response is realized. Correspondingly the flux density for the transient state is shown in Fig. 16 which varies slowly and contains a vanishing DC component. Transient currents of the primary and secondary windings of the transformer are displayed in Fig. 17-19 respectively. Comparison of Fig. 14 and 18 shows that the variations of the field intensity and primary current are somewhat similar having a big jump in the beginning of transient while there is no significant transient in the secondary current shown in Fig. 19. According to Fig. 18 the primary current becomes several times of its nominal value during 10ms of the first switching transient. This event is known as inrush current [19]. Measured primary current for a few cycles of the beginning of transient is shown in the Fig. 18 for comparing. A comparison between simulation result and experimental result given in Fig. 18 confirms the accuracy of the proposed modeling approach of this paper.

Simulation results for the above described system with no differences except the initial phase of the voltage source which is now $\varphi = \pi/2$ are given in Fig. 20-23 for comparison. A remarkable point in these figures is that the transient amplitude and period of switching at a time when the input voltage is peak are more slightly in comparison with the switching at the time of being zero voltage.

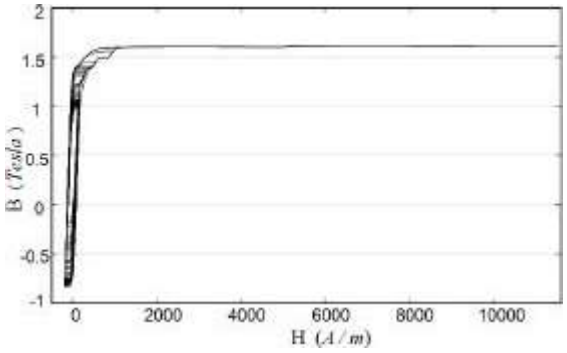

Fig. 11: Transient B-H curve of transformer core while the value of voltage is zero in switching instant

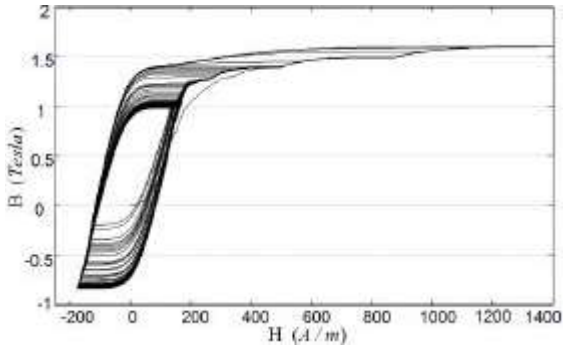

Fig. 12: Enlargement of transient B-H curve of Fig 8

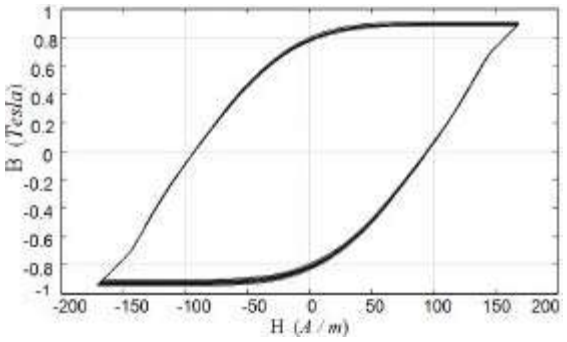

Fig. 13: B-H curve of transformer core in steady state

Harmonic contents of the steady state currents of primary and secondary windings are not easily visible without a harmonic analysis of Fig. 18 and 19. However, according to Fig. 15, the steady state field intensity is thoroughly non-sinusoidal. Harmonic content spectrum of the field intensity given by Fig. 24,

shows that the field intensity does not include the even harmonics and the higher order odd harmonics are smaller. Probably, a question came out here is that why the minor loops have not appeared on the main hysteresis loop while the field intensity contains harmonics? The answer is that according to the Preisach model, those harmonics can produce minor loops if they alter the increasing or decreasing mode of the field intensity H and create new vertices in the Preisach triangle; otherwise no minor loops will be created.

As mentioned previously the system is simulated under various inductive and capacitive loads one discussed above using the proposed modeling approach. Essentially similar results are achieved with some differences in the values of the output parameters for each load. It is noticeable that the inrush phenomena are considerable almost in all load conditions. For example, the transient current of the primary winding of the no load transformer is similar to the result given above for the inductive load but the steady currents of the primary are somewhat different. Steady state current of the primary winding under no-load condition is little but fully non sinusoid.

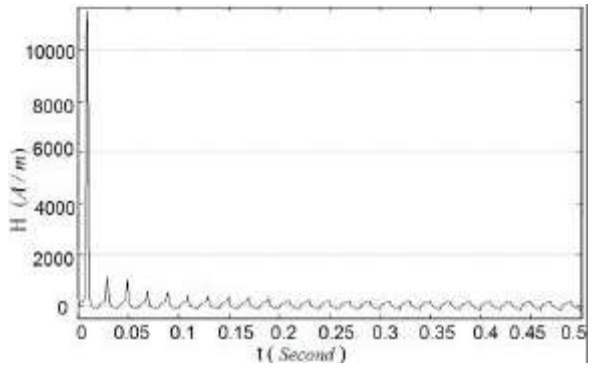

Fig. 14: Transient curve of magnetic field intensity of transformer core while the value of voltage is zero at switching instant

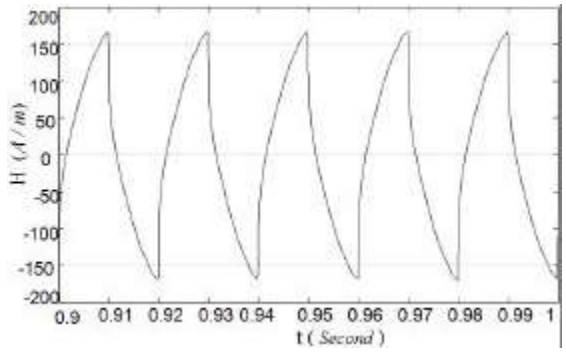

Fig. 15: Magnetic field intensity of transformer in steady state

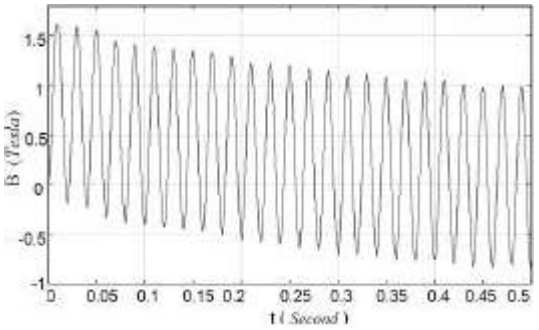

Fig. 16: Transient curve of magnetic flux density of transformer core while the value of voltage is zero at switching instant

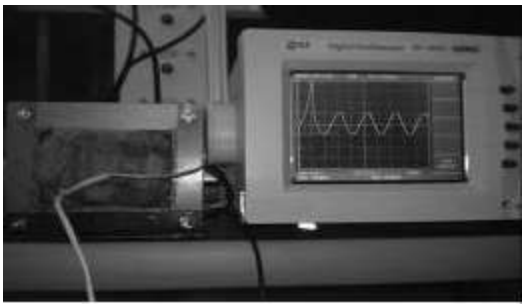

Fig. 17: Experimental transformer and inrush current

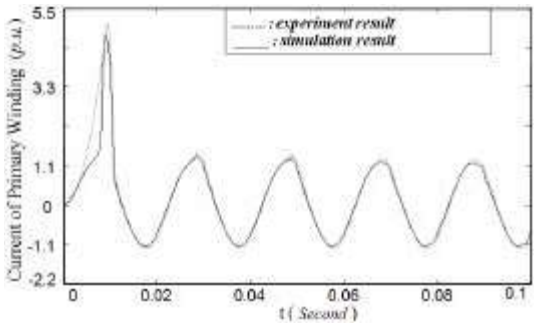

Fig. 18: Transient current of primary while the value of voltage is zero at switching instant

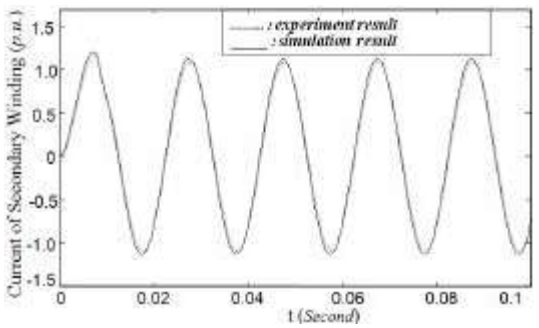

Fig. 19: Transient current curve of secondary while the value of voltage is zero at switching instant

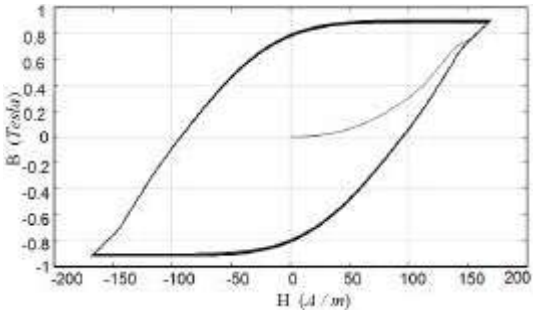

Fig. 20: Transient B-H curve while the value of voltage is maximum at switching instant

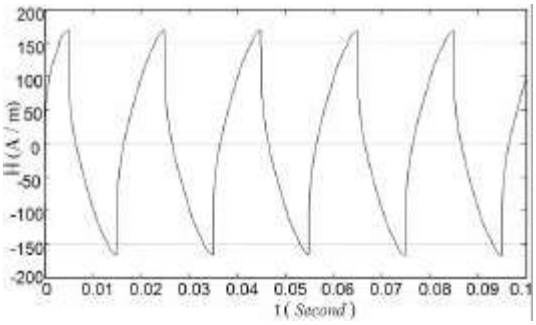

Fig. 21: Transient magnetic field intensity while the value of voltage is maximum at switching instant

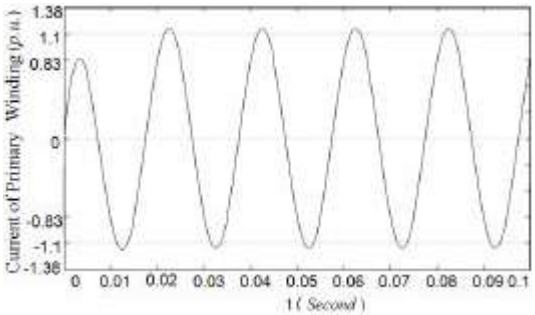

Fig. 22: Transient current of primary while the value of voltage is maximum at switching instant

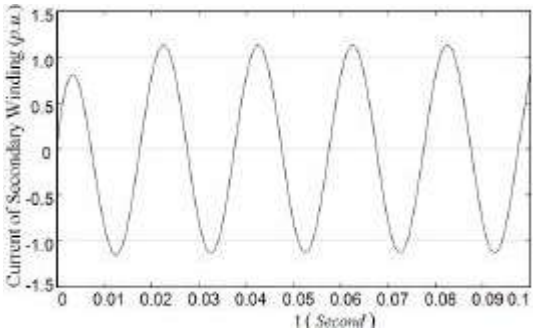

Fig. 23: Transient current secondary while the value of voltage is maximum at switching instant

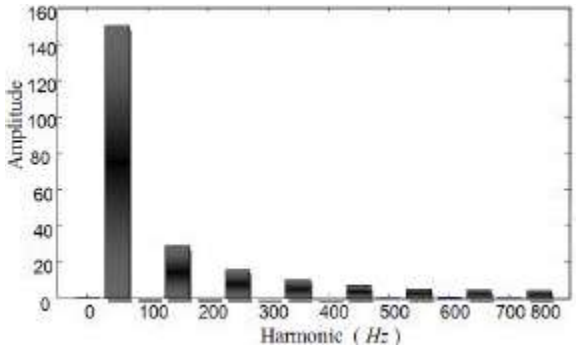

Fig. 24: Harmonic distribution of magnetic field intensity of transformer core

CONCLUSION

Accurate analysis of the steady state and transient phenomena of transformer without paying sufficient attention to the complicated, non-linear and multi-value characteristics of ferromagnetic substance is nearly impossible. The problems associated with coupling the Preisach model to the external circuits are solved in this paper properly by using a numerical algorithm. The steady state and transient performance of a transformer can be predicted by this algorithm. The algorithm is described and it is applied for a particular operating condition as an example of the modeling approach capability. It is shown that the model tracks the expecting output values very accurately. The example problem investigated in this paper is the inrush current arising during switching conditions. The simulation results show the effects of voltage switching instants on the first period transient currents of the primary and secondary winding of the transformer. It is shown that, if the applied voltage has zero value at the time of switching, the magnetic and electrical parameters of the system encounter with relatively much severe transient phenomena. Transient current of the primary involve a big jump during the first period of the switching transient while the secondary current does not endure such critical transient in almost all type switching occurrences. Moreover this paper illustrated the harmonic spectrum of an internal parameter in the steady state as an example of the model capacity to evaluate the power quality indices of the internal and external parameters.

REFERENCES

1. Juan A. Martinez and Bruce A. Mork, 2005. Transformer Modeling for Low-and Mid-Frequency Transients-A Review. IEEE Trans. Power Del., Vol: 20 (2).

2. Brandwajn, V., H.W. Dommel and I.I. Dommel, 1982. Matrix representation of three-phase n-winding transformers for steady-state and transient studies. IEEE Trans. Power App. Syst., PAS-101 (6): 1369-1378.
3. Chen, X., 2000. Negative inductance and numerical instability of the satura-ble transformer component in EMTP. IEEE Trans. Power Del., 15 (4): 1199-1204.
4. Henriksen, T., How to avoid unstable time domain responses caused by transformer models. IEEE Trans. Power Del., 17 (2): 516-522.
5. Cherry, E.C., 1949. The duality between interlinked electric and magnetic circuits and the formation of transformer equivalent circuits. In Proc. Physical Society, 62: 101-111.
6. Slemon, G.R., 1953. Equivalent circuits for transformers and machines including non-linear effects. In Proc. Inst. Elect. Eng. IV, 100: 129-143.
7. Dick, E.P. and W. Watson, 1981. Transformer models for transient studies based on field measurement. IEEE Trans. Power App. Syst., PAS-100 (1): 401-419.
8. Arturi, C.M., 1991. Transient simulation and analysis of a five-limb generator step-up transformer following an out-of-phase synchronization. IEEE Trans. Power Del., 6 (1): 196-207.
9. de León, F. and A. Semlyen, 1994. Complete transformer model for electromagnetic transients. IEEE Trans. Power Del., 9 (1): 231-239.
10. Narang, A. and R.H. Brierley, 1994. Topology based magnetic model for steady-state and transient studies for three phase core type transformers. IEEE Trans. Power Syst., 9 (3): 337-1349.
11. Mork, B.A., 1999. Five-legged wound-core transformer model: Derivation, parameters, implementation and evaluation. IEEE Trans. Power Del., 14 (4): 1519-1526.
12. Yacamini, R. and H. Bronzeado, 1994. Transformer inrush calculations using a coupled electromagnetic model. In Proc. Inst. Elect. Eng., Sci. Meas. Technol., 141: 491-498.
13. Arrillaga, J., W. Enright, N.R. Watson and A.R. Wood, 1997. Improved simulation of HVDC converter transformers in electromagnetic transient programs. In Proc. Inst. Elect. Eng., Gen. Transm. Distrib., 144: 100-106.
14. Hatziargyriou, N.D., J.M. Prousalidis and B.C. Papadias, 1993. Generalised transformer model based on the analysis of its magnetic core circuit. In Proc. Inst. Elect. Eng. C, 140: 269-278.
15. Chen, X., 1996. A three-phase multi-legged transformer model in ATP using the directly-formed inverse inductance matrix. IEEE Trans. Power Del., 11 (3): 1554-1562.
16. Zdzislaw Wlodarski, 1996. Modeling dynamic hysteresis loops and iron losses by the use of equivalent circuits. Compel, 24 (1): 158-166.
17. Mayergoyz, I.D., 1991. Mathematical models of hysteresis. New York, USA, Springer Verlag.
18. Darabi, A., M.E. Ghazi, H. Lesani and A. Askarinejad, 2007. Calculation of Local Iron Loss in Electrical Machines Using Finite Elements Method. Engineering Letters, 15:2, EL_15_2_01.
19. Ling, P.C.Y. and A. Basak, 1988. Investigation of Magnetizing Inrush Current in a Single-Phase Transformer. IEEE Trans. Magnetics., 24 (6): 3217-3222.